Journal of New Materials for Electrochemical Systems 21, 081-089 (2018)
© J. New Mat. Electrochem. Systems

ZnO-carbon Active Nanostructured Thin Film Fabrication by Spin Coating Technique for Enzymatic Urea Biosensing

Kobra Ghayedi Karimi[1,*], Mahmoud Ebrahimi[1,†] and Sayed Ahmad Mozaffari[2]

[1]Department of Chemistry, Mashhad Branch, Islamic Azad University, Mashhad, Iran
[2]Thin Layer and Nanotechnology Laboratory, Institute of Chemical Technology,
Iranian Research Organization for Science and Technology (IROST), Tehran, Iran

Received: December 04, 2017, Accepted: February 02, 2018, Available online: April 25, 2018

Abstract: *Spin coated zinc oxide (ZnO)-carbon active porous media on the Fluorine-doped Tin Oxide (FTO) coated glass is presented as an engaged nomination for novel application in enzymatic urea biosensor. Some correlations between the processing parameters spinning speed, spinning duration, volume of solution and ZnO:carbon active ratio and respective thin film characteristics were determined, then uniform ZnO-carbon active the uniform film was achieved at the optimum deposition conditions. FE-SEM was employed to investigate the morphology and hardness of ZnO-carbon active thin film. The FE-SEM image illustrates cavities of a thin film as an efficient transducer area for immobilization of urease enzyme (Urs). Stepwise study of FTO/ZnO-carbon active/Urs biosensor manufacturing was performed by voltammetric and impedimetric techniques. The results revealed a good sensitivity for impedimetric urea retrieval between 8.0-110.0 mg* dL^{-1} *with detection limit of 5.4 mg* dL^{-1}*.*

Keywords: ZnO-carbon active thin film; Urea biosensor; Spin coating; Electrochemical impedance spectroscopy

1. INTRODUCTION

Zinc oxide (ZnO), is one of the attractive semiconductor materials, has presented significant benefits including carrier mobility and direct band gap energy (3.27 eV). Furthermore, ZnO has critical applications in pigmentary, photocatalysis, photovoltaic devices, conducting coating, gas sensors, and electrostatic transducers, as a UV absorber, it can be operated in cosmetics, paints, balms, varnishes, and plastics [1]. Ample evidence has been provided indicating that ZnO strongly influences the shape and size properties also utilization of materials. Thus, a lot of effort has been devoted to control its particle size and shape; however, its control within the base of nanoparticle synthesis science is still a challenging issue. Several parameters containing time, temperature, precursors, concentration, and solvents are established to effect the shape and size of nanoparticles. Influence of *metal oxide nanoparticles* is an interesting topic because there can be a type of complex morphologies in this regard [2]. Over recent years, some of its features have been specified [3,4]. For the broad variety of applications, numerous ZnO thin film preparation techniques have been attempted: sol-gel [5], electrophoreses [6], hydrothermal [7], and sputtering [8,9] techniques. Although there are comparatively few results on the spin coating fabrication of ZnO thin films. Some nanostructured metal oxide including ZnO has been utilized for enzymes immobilization for accelerated electron transfer among active sites of enzyme and electrode [10]. Alternative electrochemical biosensors are remarkably attended to due to their for simplicity, good sensitivity [11], inexpensive, large surface area to volume ratio, excellent choice, and electrical properties. Among a great deal of enzymes applied in biosensor construction, a urease enzyme-based sensor displays a desperate role in detecting urea.

Urea formula is $CO(NH_2)_2$. A urea molecule has two -NH_2 groups joined by a carbonyl group (C = O) [12]. Urea is solid, white, odorless, non-toxic, and good solubility in water. Moreover, it is important in metabolism of nitrogen-containing compounds. Urea is widely distributed in nature and is generally applied in clinical chemistry and biochemistry with special attention [13]. The normal range of urea in blood serum is from 15-40 mg dL^{-1}. Increasing in urea level in blood and urine can cause urinary tract obstruction, dehydration, shock and gastrointestinal bleeding, whereas reducing in urea level may be noticed in nephrotic syn-

To whom correspondence should be addressed:
Email: * karimi277@yahoo.com, †ebrachem2007@yahoo.com

drome and hepatic failure [14]. The assay of urea can be followed by other techniques as amperometry [15], potentiometry [16], spectrometry [17], and conductometry [18]. At the present time, numerous types of electrochemical biosensors are made for tracing of urea with application of urease in urea hydrolysis process employed in potentiometric evaluation [19,20]. Potentiometric biosensors suffer from number of difficulty including slow response times and interference effect by Na^+ and K^+ [21,22]. Therefore, several techniques have been recommended to determine urea as non-potentiometric urea-based assessment procedures [23,24].

Electrochemical impedance spectroscopy (EIS) can be considered as a powerful technique to study the electrical attributes of biosensing interfaces. Moreover, impedimetric assessment as a speed, sensitive, and repeatable style can be employed to consider urea via an electrochemical signal transduction [25-28].

As well as ZnO part of transducer, carbon active as other part was consumed for construction of transducer surface of biosensors due to their exclusive ability to facilitate electron transfer among the electrode and active site of the required enzyme.

The ZnO-carbon active surface transducer construction has a vital effect on analytical efficiency of urea biosensor. Activated carbon is highly porous carbon with good surface area. It is a usual approximation that 1 gram of activated carbon has a surface of approximately 1000 to 3000 square meters. Activated carbon, also called amorphous carbon, is mostly used in supercapacitor electrode interests [29]. Spin coating method applied to formation a uniform ZnO/carbon active hybrid uniform film on flat substrates.

In this work, a simple way of FTO/ZnO-carbon active/Urs biosensor was made by apply of ZnO-carbon active uniform film as an excellent platform for immobilization of enzyme for the appropriate transducer conductivity. The impedimetric method was applied to evaluate urea by FTO/ZnO-carbon activate/Urs biosensor. The fast response time fewer than 10 seconds for FTO/ZnO-carbon active/Urs biosensor was obtained. Moreover, enzymatic activity was retained holding for more than 3 weeks at 4 °C in the storage and non-use conditions.

2. EXPERIMENTAL

2.1. Apparatus and materials

The deposition of ZnO-carbon active thin films was performed in spinner system (IROST, Tehran, Iran). The surface probing of uniform film was performed using a Tescan Mira II FE-SEM. Impedimetric and Voltammetric tests were done with a potentiostat/galvanostat (PGSTAT. 302N, Autolab, Eco-Chemie, The Netherlands). All electrochemical tests were constructed in a formal three electrode system at ambient temperature. FTO/ZnO-carbon active/Urs electrode applied as working electrode (surface area=1cm^2), Pt and SCE electrodes SCE and Pt electrodes were applied as reference and counter electrodes, respectively. An electrochemical cell was placed in a Faraday cage to eliminate any environmental stray effects. For EIS measurements, 10 mV peak-to-peak ac amplitude was used an amplitude of frequencies from 10 mHz to 100 kHz was scanned, and the impedances were registered. EIS data analysis using Zview/Zplot (Scribner Associates, Inc.) was according to the algorithm of Macdonald's (LEVM 7), using a complex non-linear least square (CNLS) approximation method [31].

Urs (urease enzyme, E.C.3.5.1.5 Jack Bean), urea (ACS represent 99.9%), and all chemical reagents used in this project were of analytical reagent grade and purchased from Sigma-Aldrich. Fluorine-doped Tin Oxide (FTO) coated glass purchased from Dyesol Company. Phosphate buffer solution (PBS) was provided from K_2HPO_4 and KH_2PO_4, with pH at 7.4. Urs solution was prepared in PBS, 0.1 M, pH 7.4 containing 100 U mg^{-1} for 30 minutes. A stock solution of urea was provided in 0.1 M PBS, and stored at 4 °C. The low concentration standard solution of urea was freshly applied for each experiment.

2.2. ZnO nanoparticles preparation

A stock solution 3.0 M NaOH (pH=13.0) and 0.3 M $ZnSO_4$ (pH=5.0) were made. The reactions were performed with continuously stirring the stock solution of $ZnSO_4$ along with the highly base solution of NaOH. After the mixing of the solutions, the mixture was placed on hot plate at 110 °C for 2 h to permit precipitation. The precipitated products was centrifuged, and washed with double distilled water and so dried at 400 °C for 20 min.

2.3. Fabrication of FTO/ZnO-carbon active hybrid film by spin coating

The principal purpose of this experimental study was addressing the perform of spin coating parameters such as spinning speed, volume of solution, spinning duration, and ZnO:carbon active ratio on resistance of prepared thin films. In rule of obtain very uniform thin film, four sets of depositions parameters were accomplish at various spinning speed (500 to 2500 rpm), volume of solution (0.1 to 0.9 ml), spinning duration (10 to 50 s), and precursor ZnO:carbon active ratio (10:1 to 1:1 g.L^{-1}). In every set of samples, only one of the above-mentioned parameters was varied while keeping other parameters constant. Spinning speed has been shown to have great influences on many physical properties, such as film thickness, electrical resistance and mechanical properties. In this project, the spin coating conditions are selected to be optimum for ZnO-carbon active formation of uniform film with the least electrical resistivity.

In Figure. 1a the dependence of ZnO-carbon active thin film electrical resistivity on spinning speed (500 to 2500 rpm) is shown. Increasing of spinning speed to 2000 rpm resulted in decreasing in electrical resistivity of thin film. Decreasing film thickness following by spinning speed to 2000 rpm causes uniform structure while increasing spinning speed up to 2500 rpm produces a slightly non-uniform thin film because of high centrifugal force. The result was exhibited a non-linear relationship between spinning speed and electrical resistivity of thin film. Figure. 1b illustrates reduce of the resistivity with increase in the volume of solution from 0.1 to 0.7 ml, and no sensible change up to 0.9 ml, then 0.7 ml selected as an optimum volume of solution. Figure. 1c shows that the coating thickness decreased with increase in spinning duration from 10 to 40 s and no sensible change up to 50 s. During the first seconds, in less than forty seconds, only a portion of substrate to be coated is covered and is not spread uniformly.

The precursor ZnO:carbon active ratio is very effective parameter in spin coating for obtaining the nanoporous obtaining the ZnO-carbon active thin film with lower electrical resistivity and the suitable substrate for Urs enzyme immobilization. By increasing the amount of carbon active in precursor ZnO:carbon active ratio, the lower electrical resistivity of thin film will be observed (Figure.

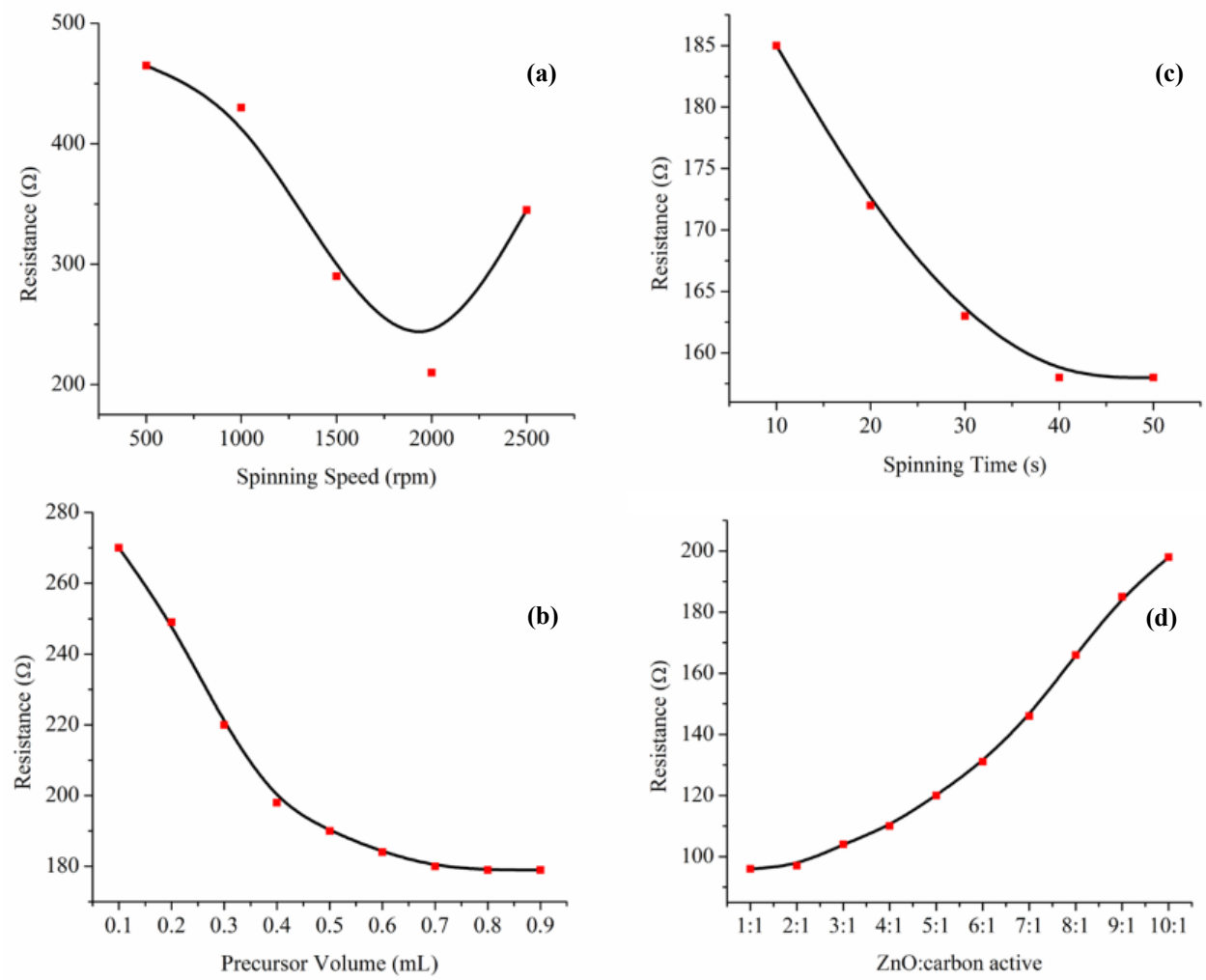

Figure 1. Effect of spinning speed (a), volume of solution (b), spinning duration (c), and ZnO:carbon active ratio (d) on ZnO-carbon active film resistivity.

1d). This behavior demonstrates the raising or reducing effect of carbon active amount in the ZnO:carbon active ratio on the formation of semiconductor:conductor phases in the thin film, which finally refers to higher or lower electrical resistivity of uniform film. Further, the precursor ZnO:carbon active ratio has a vital effect in Urs with immobilization of enzyme ZnO part, so precursor 5:1 ZnO:carbon active ratio was selected.

The optimum conditions for obtaining uniform nanoporous ZnO-carbon active thin film were considered in continue as 2000 rpm, 0.7 ml, 40 s and 5:1 for spin coated spinning speed, the volume of solution, spinning duration, and ZnO:carbon active ratio, respectively. The periodic and continuous annealing of ZnO-carbon active thin film at 400 °C cause better aligned textured films which are needed for a homogeneous matrix for immobilization of enzyme in biosensor structure.

2.4. Fabrication of FTO/ZnO-carbon active/Urs biosensor

Enzyme immobilization appear as a key factor to expand effective biosensors with suitable efficiency such as storage stability, fast response time, high sensitivity, good selectivity, and reproducibility. Urs was immobilized by soaking the FTO/ZnO-carbon active electrode in PBS, 0.1 M, pH 7.4 containing 100 units of Urs for 30 min at ambient temperature. The FTO/ZnO-carbon active/Urs electrode was then washed and kept in PBS until use. Stepwise observation of FTO/ZnO-carbon active/Urs biosensor manufacturing was accomplished applying electrochemical techniques as well as current *vs.* potential (I-V curve), EIS and CV techniques. After completing these steps, biosensors as working electrode was applied for detection of urea using impedimetric measurements.

3. RESULTS AND DISCUSSION

3.1. UV transmission spectrum and morphological characterization of spin coated ZnO carbon active thin film

The recorded transmission spectrum for ZnO-carbon active thin film is illustrated in Figure. 2. The sharp absorption onset and the high transmission values at wavelengths above 320 nm exhibit the

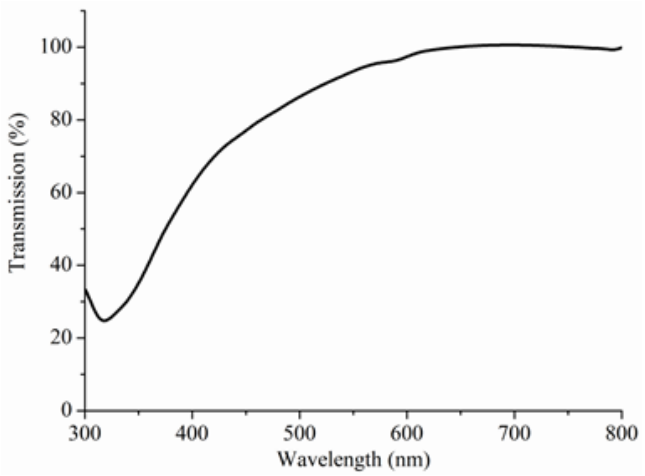

Figure 2. UV transmission spectrum recorded for ZnO nanoparticle.

low concentration of defects such as pits and voids of the ZnO thin film.

The surface morphology characterization of nanoporous ZnO-carbon active thin film was illustrated by FE-SEM (Figure. 3a). Uniform pores display a main role in enzyme immobilization. As well as, the distribution of zinc oxide nanoparticles provides high surface area which can lead to being more of an immobilized enzyme on the surface (Figure. 3b).

3.2. Impedimetric and voltammetric characterization of fabricated biosensor in the absence/presence of urea

Figure. 4a and 4b present the impedance pectra and cyclic voltammetry studies. Nyquist plots (-*Z*'' *vs.* *Z*') and voltammograms are provided, as well. The layer by layer assembly of FTO/ZnO-carbon active/Urs in a solution of urea-free PBS containing 5.0 mM $[Fe(CN)_6]^{3-/4-}$ is also presented. Monitoring the assembled layer by layer biosensors in the whole EIS spectrum and cyclic voltammogram was performed with the display of a semicircle part corresponding to the charge transfer resistance (R_{ct}) and the ranging anodic peak current (i_{pa}) of the marker ($[Fe(CN)_6]^{3-/4-}$) in the electrolyte solution, respectively.

Three layers of (a) FTO, (b) FTO/ZnO-carbon active, and (c) FTO/ZnO-carbon active/Urs result in a change of the electron-transfer resistance and amplitude of i_{pa} from (a) R_{ct} =0.96 kΩ, i_{pa}=2.09 mA to (b) R_{ct} =3.3 kΩ, i_{pa}=0.81 mA and (c) R_{ct} =4.70 kΩ, i_{pa}=0.41 mA, respectively. The R_{ct} and i_{pa} values of ZnO-carbon active film (Figure. 4a and 4b; curve b) with respect to FTO electrode (Figure. 4a and 4b; curve a) is changed, which is dependent to the lower electrical conductivity of ZnO-carbon active nanoporous film respect to FTO layer. In other way, the R_{ct} value further increases and i_{pa} value decreases (Fig. 4a and 4b; curve c) after the immobilization of Urs onto FTO/ZnO-carbon active electrode because of insulating specifications of Urs. By comparing curve b and c in Figure. 4a and 4b which represent the EIS and CV spectra of $[Fe(CN)_6]^{3□/4-}$ redox reaction at FTO/ZnO-carbon active and FTO/ZnO-carbon active/Urs electrodes, it can be noticed that Urs

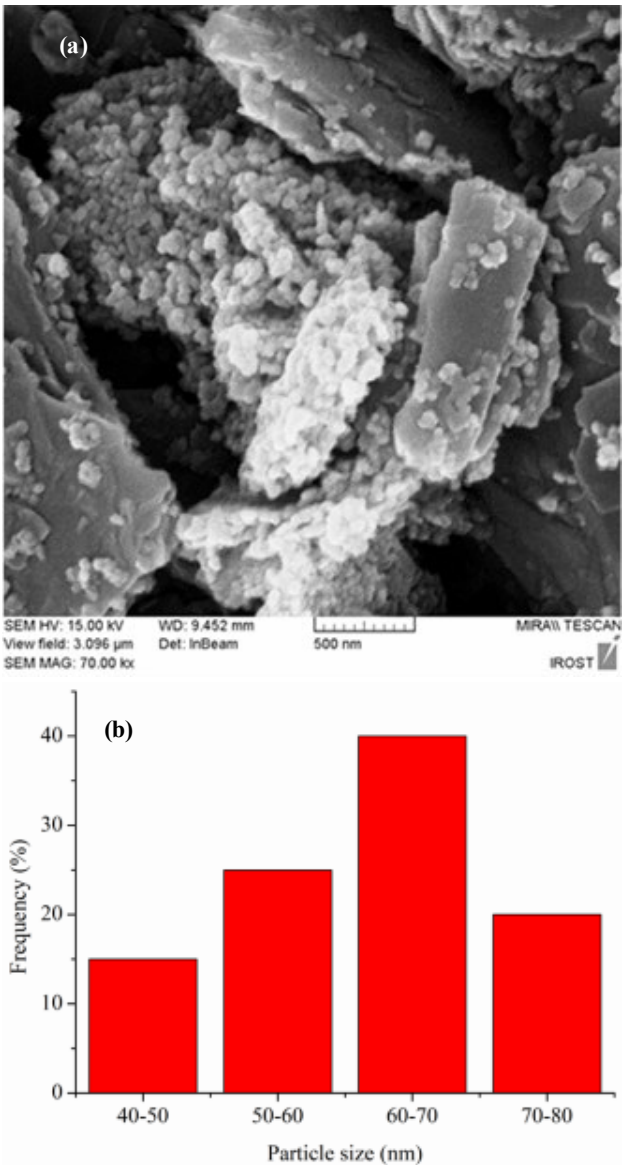

Figure 3. FE-SEM images of deposited ZnO-carbon active thin film (a), and the particle size distribution histogram (b).

layer decreases direct electron transfer of $[Fe(CN)_6]^{3□/4-}$ redox probe with electrode substrate measure with ZnO-carbon active thin film.

The R_{ct} and i_{pa} values (Figure. 5a and 5b) at the interface of the FTO, FTO/ZnO-carbon active, FTO/ZnO-carbon active/Urs biosensor in the presence of 110.0 mg dL^{-1} urea were studied by applying EIS and CV techniques, respectively. The R_{ct} and i_{pa} values at ZnO-carbon active thin film (R_{ct}=38 kΩ, i_{pa}=0.02 mA, curve b) evaluate with the values were obtained at FTO electrode (Figure. 5a and 5b; curve a) involve to represents a partial hydrolysis of urea at ZnO-carbon active thin film. Further decreasing in R_{ct} and increasing in i_{pa} values (R_{ct}=8.5 kΩ, i_{pa}=0.11 mA, curve c) were monitored after Urs immobilization onto FTO/ZnO-carbon active matrix due to fast hydrolysis of urea by the enzyme.

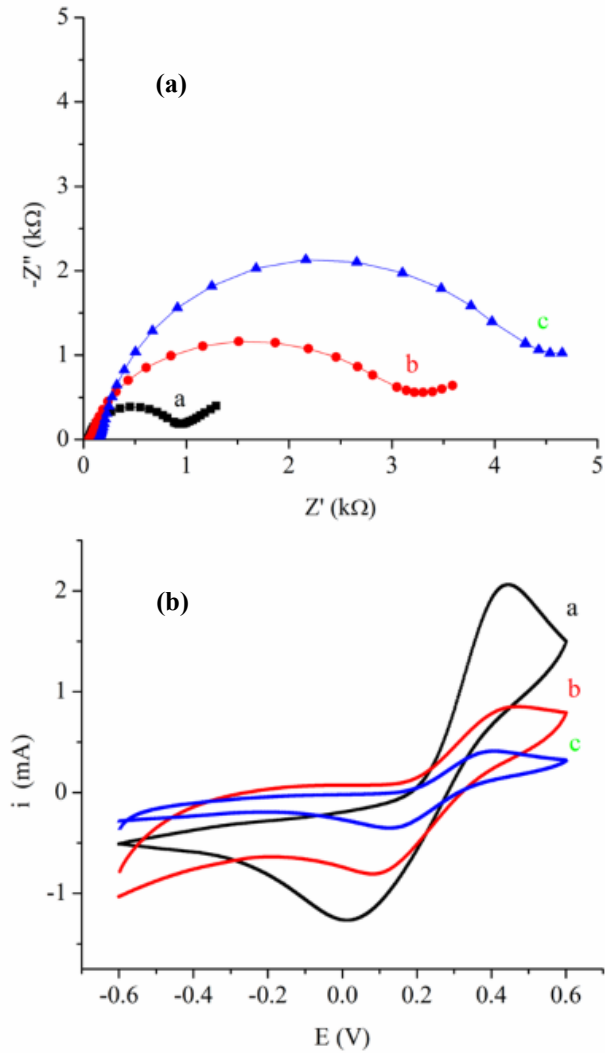

Figure 4. (a) The Nyquist plots (-Z'' *vs.* Z') obtained in urea□free PBS (pH 7.4) containing 5 mM $[Fe(CN)_6]^{3-/4-}$ on (a) FTO, (b) FTO/ZnO-carbon active, and (c) FTO/ZnO-carbon active/Urs. (b) Cyclic voltammogram obtained in urea□free PBS (pH 7.4) containing 5 mM $[Fe(CN)_6]^{3-/4-}$ on (a) FTO, (b) FTO/ZnO-carbon active, and (c) FTO/ZnO-carbon active/Urs at the scan rate of 0.1V s^{-1}.

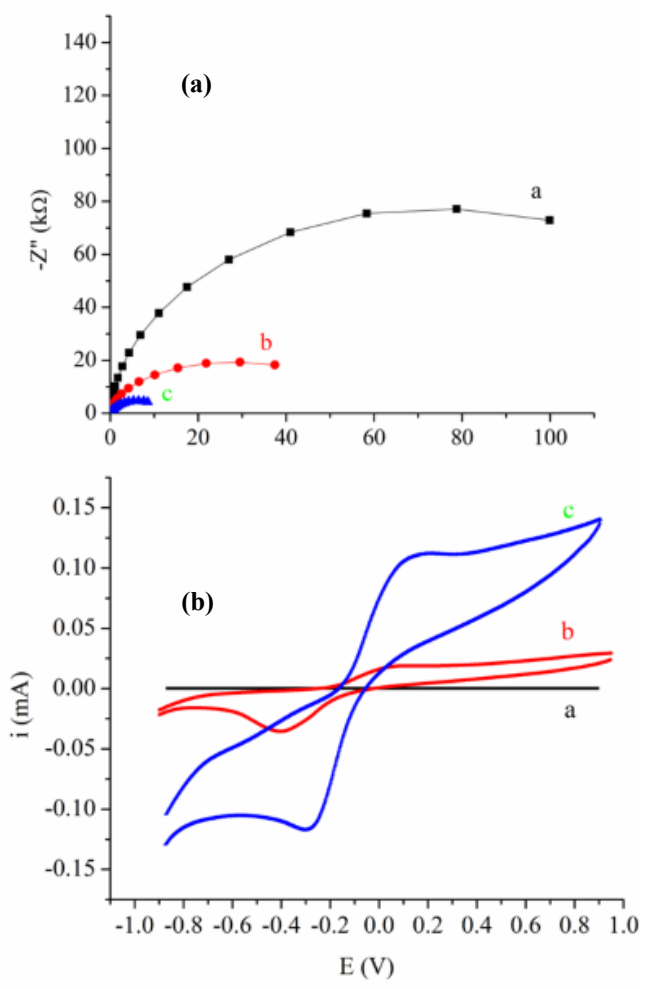

Figure 5. (a) The Nyquist plots (-Z'' *vs.* Z') obtained in PBS (pH 7.4) containing 110 mg dL^{-1} urea on (a) FTO, (b) FTO/ZnO-carbon active, and (c) FTO/ZnO-carbon active/Urs. (b) Cyclic voltammogram obtained at at the scan rate 0.1 V s^{-1} in PBS (pH 7.4) containing 110 mg dL^{-1} urea on (a) FTO, (b) FTO/ZnO-carbon active, and (c) FTO/ZnO-carbon active/Urs.

3.3. Determination of enzyme activity after immobilization

The electrical property of FTO/ZnO-carbon active/Urs was studied to determine the enzyme activity after Urs immobilization. For this measurement, a cell was made, which consists of gold wire (Φ 0.3 mm, 5 cm length) as an electrode and FTO/ZnO-carbon active/Urs as another electrode. Potential from 0.0 to 1.0 V was applied to the film and the corresponding dc current was determined. For each sample, four sets of measurement were done at ambient temperature. Urea solutions with several concentrations of urea such as 0, 8.0, 60.0 and 110.0 mg dL^{-1} were prepared in PBS and used as an electrolyte. The amount of 10 ml electrolyte was used for all measurements. While the urea concentration in PBS was changing, the conclusion of urea enzyme activity could be displayed on the curve. As shown in Figure. 6, the slope of I-V curve ($\Delta I/\Delta V$) is a scale of enzyme activity of the biosensor.

The increasing in the sample current is clear after immobilization (Figure. 6b). Although urea can directly react with zinc oxide, reaction kinetics of Urs...urea is various from that of ZnO...urea. This reaction is not the similar as its reaction after immobilization of enzymes. The purpose of several urea concentrations can be observed on the curve of enzyme activity. By adding the urea concentration, the enzyme activity increased, as well.

3.4. Expected Sensing mechanism

Figure. 7 illustrates the diagram of expected sensing mechanism. Initially, atmospheric oxygen molecules were physisorbed on the surface sites by extracting electrons from the transition band while moving them from one site to another, as a result of which they

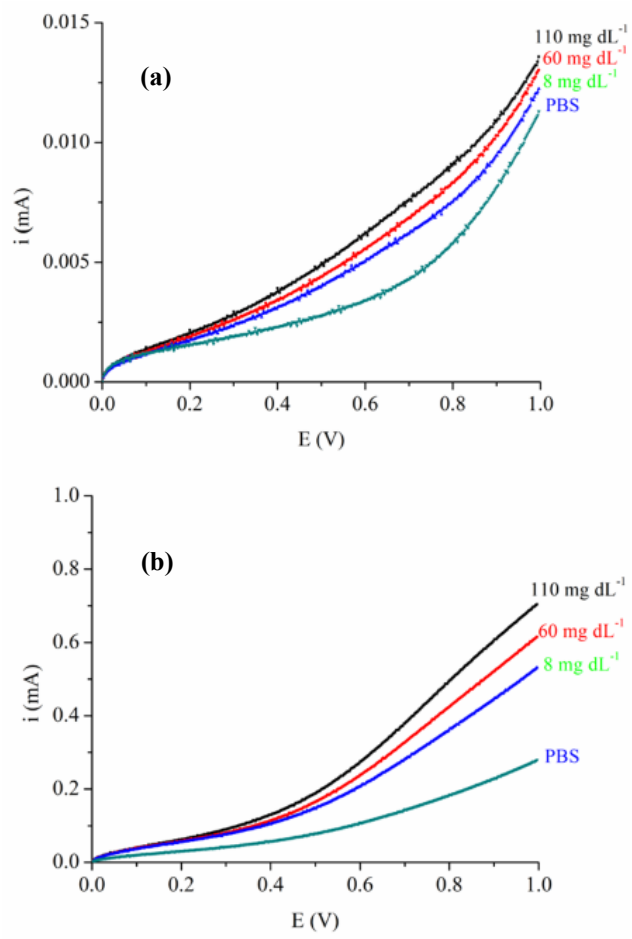

Figure 6. The I-V curves showing the effect of Urs immobilization on ZnO-carbon active films with increasing urea concentration, (a) before and (b) after Urs immobilization.

were ionosorbed on the similar level as O_{ads}^-. This process led to a reduction in the conduction of transducer conversion, as a result of an increase in the potential barrier at the grain boundaries (Figure. 7a).

Upon exposing FTO/ZnO-carbon active/Urs to urea, an enzymatic reaction takes place between Urs and urea which can be, represented as below equation:

$$NH_2CONH_2 + 2H_2O \xrightarrow{Urs} 2NH_4^+ + CO_3^{2-} \quad (1)$$

At first NH_4^+ from uncharged urea which raises the conductivity of the FTO/ZnO-carbon active/Urs by providing the excess electron to the conduction band. Further, as demonstrated in the below reaction when reducing gas (R) molecules (released ammonia by enzymatic hydrolysis of urea in the present case) reaction with oxygen that attracts the negatively charged electron adsorbates, the trapped electrons were given back to the transition band of ZnO (Figure. 7b) [32].

$$R + O_{ads}^- \longrightarrow RO + e^- \quad (2)$$

The conclusions get by CV (Figure. 5b) were listed on the sensing mechanism, which clearly points to an oxidation and reduction process. For further evidence to validate our suggested biosensing mechanism, the impedimetric response of FTO/ZnO-carbon active by NH_3 concentration was evaluated in a urea-free NH_3 solution. As shown in Figure. 8, by increasing, concentration of NH_3 from 0.001 to 0.01 M, the magnitude of R_{ct} decrease. When reducing molecules (R = ammonia) reacts with pre-adsorbed negatively charged oxygen adsorbates (Eq. 2), the trapped electrons are given back to conduction band of ZnO, and slightly decrease of R_{ct} is observed. The results obtained by impedimetric studies of R_{ct} difference as a function of NH_3 concentration support the proposed mechanism.

3.5. Impedimetric assessment

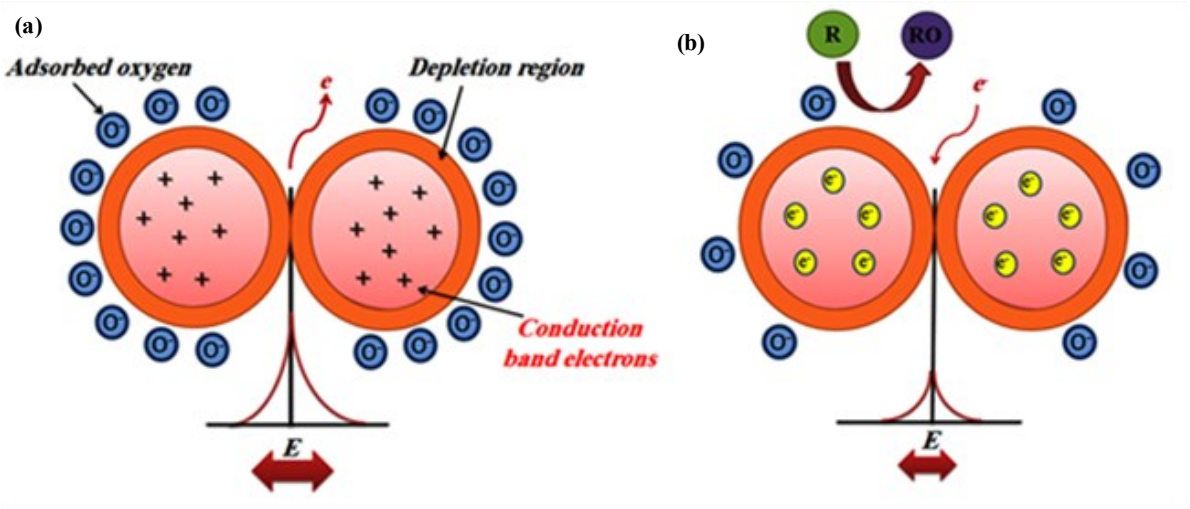

Figure 7. The proposed mechanism of urea sensing on the ZnO-carbon active surface in the **(A)** absence, and **(B)** presence of a reducing gas (R).

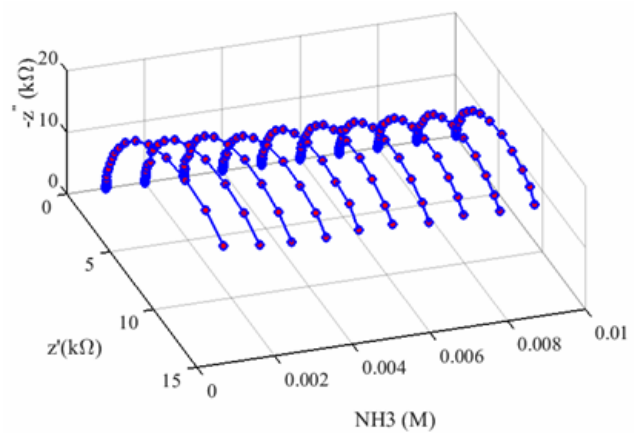

Figure 8. The Nyquist plots (-Z'' *vs.* Z') obtained on the FTO/ZnO-carbon active electrode in the presence of different concentration of NH_3.

The electrochemical response of FTO/ZnO-carbon active/Urs biosensor has been impedimetrically evaluated as a dependent factor of urea concentration. The modified Randles equivalent circuit was explained to approach the EIS data in the presence of urea (Figure. 9a). As shown in Figure. 9b, the magnitude of R_{ct} decreases on by increasing of urea concentration from 8.0 to 110.0 mg dL^{-1} ammonia in the present case. The quick response implies that the porosity of ZnO-carbon active matrix yields a low-mass transfer barrier and a rapid diffusion from solution to the enzyme while keeping its bioactivity. At physiological pH (pH=7.4), ZnO IEP~9 possess a positive charged surface which prepared a suitable microenvironment for negatively charged urease (IEP~5.9) to retain its activity [32].

The impedimetric studies obviously showed a trend of reversible process and approved Urs...urea enzymatic catalysis. Impedimetric studies and the step by step investigation established that the sensor can be re-used. The calibration curve was obtained for urea at the FTO/ZnO-carbon active/Urs biosensor by monitoring its R_{ct} responses ($|\Delta R_{ct}|=|R_{ct\ urea}-R_{ct\ buffer\ (blank)}|$). Figure. 9c displays a working curve shown in a linear scale [ΔR_{ct} (kΩ) = 15.31 (±0.05) + 0.49

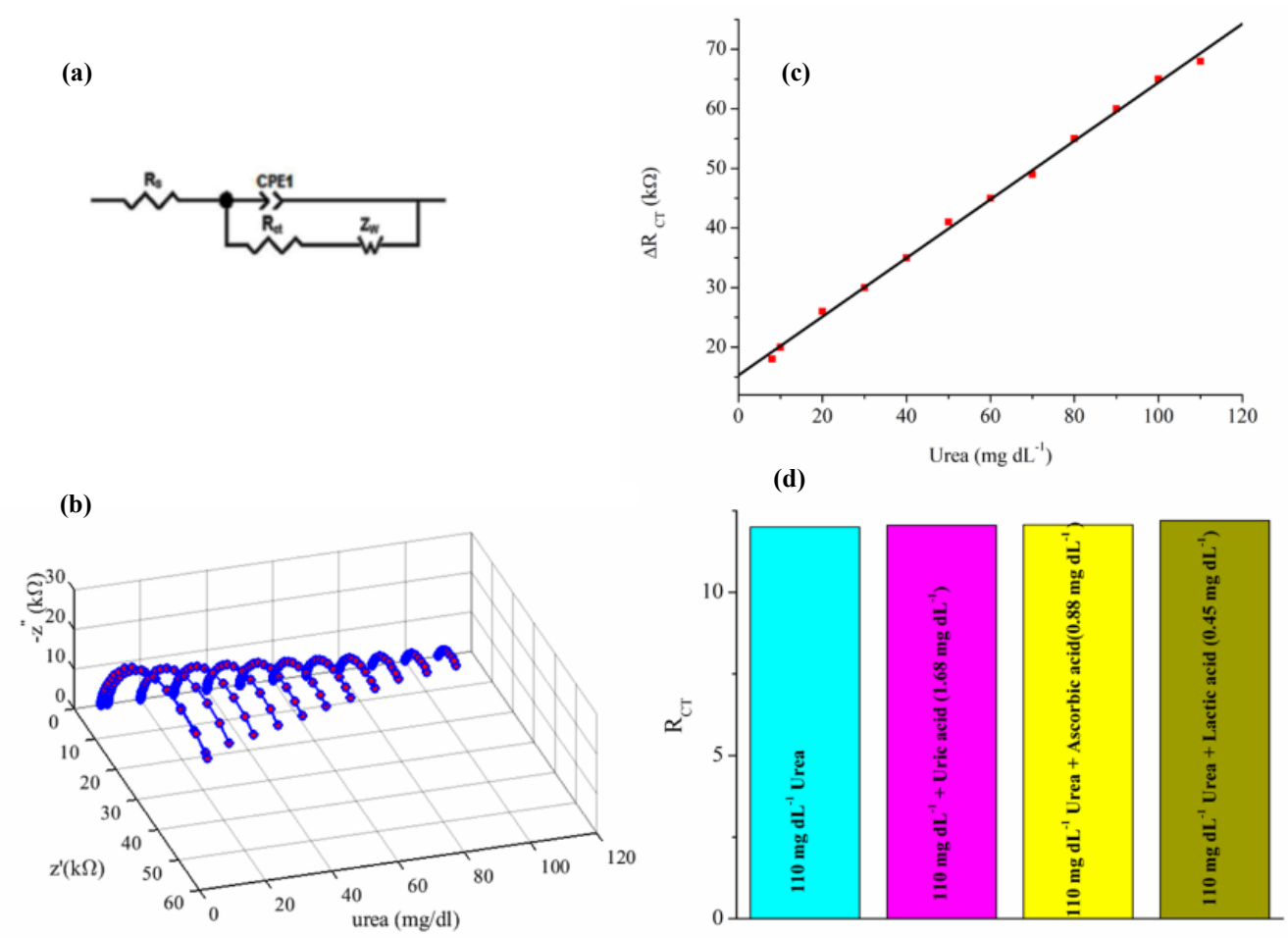

Figure 9. (a) Equivalent circuit used for impedance data approximation, (b) Nyquist plots (-Z'' *vs.* Z') obtained on the FTO/ZnO-carbon active/Urs biosensor in the presence of different concentration of urea from 8.0 to 110.0 mg dL^{-1}. (c) Variation of charge transfer resistance (ΔR_{ct}) as a function of urea concentration which represents calibration curve. (d) The graph shows the interferents effect on the response of FTO/ZnO-carbon active/Urs biosensor.

(±0.01)×[urea] (mg dL^{-1}); R^2=0.9960] in a detection range of 8.0 to 110.0 mg dL^{-1} of urea. The FTO/ZnO-carbon active/Urs biosensor displays limit of detection 5.4 mg dL^{-1} for urea and a linear range within 8.0-110.0 mg dL^{-1} with sensitivity of 0.49 kΩ per mg dL^{-1}. In order to study the selectivity of FTO/ZnO-carbon active/Urs biosensor towards the measurement of urea, EIS investigation have been performed by adding the normal concentration of the possible interferents present in human blood serum along with the concentration of urea (110 mg dL^{-1}). The EIS analysis for full of the interferents was shown in Figure. 9d, showing a maximum interference of 2% with the attendance of ascorbic acid. The effects display the significance of prepared biosensor (FTO/ZnO-carbon active/Urs) in selective detection of urea. Several assays were made on blood serum to experiment the precision of the FTO/ZnO-carbon active/Urs biosensor. Urea concentration was measured in human serum (Table 1). The relevant test was accomplished with a spectrophotometer in a local hospital. Good precision and accuracy were considered between the conclusions presented by two methods; however, the present method can be proposed for utilization in actual samples due to its good precision.

The proposed FTO/ZnO-carbon active/Urs biosensor has a fast reply time lower than 10 second and retained good enzymatic activity more than 3 weeks when kept at 4 °C temperature and not in use. Furthermore, the stability of the FTO/ZnO-carbon active/Urs biosensor was examined by evaluation the catalytic sufficiency to the urea with different storage time in 4 °C. For a constant concentration of urea, three same biosensors lost about 0.0%, 5.0% and 9.0% of their original activity after storing time of 1 day, 13 days and 6 weeks, respectively.

Table 2 evaluated analytical characteristics of the FTO/ZnO-carbon active/Urs biosensor with other biosensors. In the present study, biosensor evidently shows good response time, good limit of detection, and linear range in comparison with results of already conducted studies [33-45].

4. CONCLUSIONS

The amount of immobilized enzyme which is dependent to the surface porousity of matrix, and the matrix resistivity which is providing rapid electron transfer from immobilized enzyme to the electrode, have the significant effect in biosensor characteristics. In this work, spin coated nanoporous ZnO-carbon active thin film with excellent uniformity has been applied as a transducer media for making of the electrochemical urea biosensor via immobilization of Urs. The benefits of the spin coating procedure are its simplicity and relative ease of apply as the desired surface can be covered with a thin and uniform coating. The FTO/ZnO-carbon active/Urs biosensor was made low detection limit, good sensitivity, wide detection range, quick response time, high stability, and reproducibility by retaining enzyme activity. Impedimetric analysis of the suggested biosensor showed a fast response time lower than 10 seconds with a board dynamic range within 8.0 to 110.0 mg dL^{-1} and low detection limit 5.4 mg dL^{-1} for urea.

5. ACKNOWLEDGEMENTS

S.A. Mozaffari acknowledges the support rendered by the Iranian Research Organization for Science and Technology (IROST), and Iran Nanotechnology Initiative Council (INIC) for this research.

REFERENCES

[1] H.F. Hussein, Gh.M. Shabeeb and S.Sh. Hashim, J. Mater. Environ. Sci., 4, 423 (2011).

[2] Ph.B. Khoza, M.J. Moloto and L.M. Sikhwivhilu, J. Nanotechnol., 2012, 1 (2012).

Table 1. Determination of urea level in blood serum

Method	Sample number				
	1	2	3	4	5
Determined by Spectrophotometry (mg dL^{-1})	15.0[a]	25.9	21.1	40.0[b]	17.5
Measured by FTO/ZnO-carbon active/Urs (mg dL^{-1})	15.1	25.7	20.9	40.1	17.6
R.S.D[a] (n=5) (%)	1.2	1.0	2.0	1.1	1.3

[a]R.S.D: Relative Standard Deviation, [b]Represents the hyper- or hypo-level of urea in blood serum, the normal urea level in blood serum is between 15-40 mg dL^{-1}.

Table 2. Analytical characteristics of FTO/ZnO-carbon active/Urs compared with the values of other reported urea biosensors based on Urs physical immobilization strategy

Matrix	Response Characteristics			Stability (life time)	Detection method	Ref.
	DR	DL	RT			
Whatman paper	10-99 mg dL^{-1}	10 mg dL^{-1}	2 min	-	Potentiometric	[33]
Nano-porous silicon	10-100 mmol L^{-1}	-	<1 min	-	Amperometric	[34]
Graphite and platinum composite electrode	10-250 μM	3 μM	2 min	3 months	Amperometric	[35]
Carboxylic poly (vinylchloride)	10^{-5}-10^{-1} M	0.28 mM	-	-	Potentiometric	[36]
Nanoporous Alumina	0.5 μM-3.0 mM	0.2 μM	30 s	1 month	Conductometric	[37]
Tetramethylorthosilicate (TMOS)	0.01-30 mM	52 μg mL^{-1}	-	25 days	Potentiometric	[38]
ZnO nanoparticles	10-80 mg dL^{-1}	13.5 mg dL^{-1}	-	3 weeks	Cyclic Voltammetry	[39]
NiO nanoparticles	0.83-16.65 mM	21.3 μA	5 s	20 weeks	Cyclic Voltammetry	[40]
Mn^{2+} doping in TiO_2 thin films	0-6.5 mg mL^{-1}	-	-	-	Chronoamperometry	[41]
Silicalite	5-850 μM	-	3 min	10 days	Conductometric	[42]
BSA embedded surface modified polypyrrole film	6.6×10^{-6}-7.5×10^{-4}M	-	70-90 s	2 months	Potentiometric	[43]
TiO_2 film	8 μM-3 mM	5 μM	25 s	1 month	Potentiometric	[44]
ZnO nanorods	0.001-24.0 mM	10 μM	-	20 weeks	Cyclic Voltammetry	[45]
Spin coated ZnO-carbon active	8-110 mg dL^{-1}	5.4 mg dL^{-1}	10 s	3 weeks	Impedimetric	[This Work]

Detection Range [DR], Detection Limit [DL], Response Time [RT]

[3] S.A. Kamaruddin, M.Z. Sahdan, K.-Y. Chan, M. Rusop and H. Saim, J. Nanosci. Nanotechnol., 10, 6419 (2010).
[4] E. Bacaksiz, M. Parlak, M. Tomakin, A. Ozcelik, M. Karakiz and M. Altunbas, J. Alloys Compd., 466, 447 (2008).
[5] S.A. Kamaruddin, K.Y. Chan, M.Z. Sahdan, M. Rusop and H. Saim, J. Nanosci. Nanotechnol, 10, 5618 (2010).
[6] L. Miao, S. Cai and Z. Xiao, J. Alloys Compd., 490, 422 (2010).
[7] N.J. Ridha, A.A. Umar, F. Alosfur, M.H. Jumali and M.M. Salleh, J. Nanosci. Nanotechnol., 13, 2667 (2013).
[8] H.S. Al-Salman and M.J. Abdullah, Sens. Actuators. B, 181, 259 (2013).
[9] Q. Humayun, M. Kashif and U. Hashim, J. Nano Mat., 2013 , 1 (2013).
[10]A.A. Ansari, A. Kaushik, P.R. Solanki and B.D. Malhotra, Electrochem Commun., 10, 1246 (2008).
[11]Rajesh, V. Bisht, W. Takashima and K. Kaneto, Biomaterials., 26, 3683 (2005).
[12]C.R. Sant Ana Filho, A.L.R.M. Rossete, C.R.O. Tavares, C.V. Prestes and J.A. Bendassolli, Brazilian J. Chemical Eng., 29, 795 (2012).
[13]J. Traynor, R. Mactier and C. Geddes, BMJ., 333, 733 (2006).
[14]M. Singh, N. Verma, A.K. Garg and N. Redhu, Sens. Actuators. B, 134, 345 (2008).
[15]I. Bozgeyik, M. Senel, E. Cevik and M.F. Abasiyanik, Curr. Appl. Phys., 11, 1083 (2011).
[16]B. Lakard, D. Magnin, O. Deschaume, G. Vanlancker, K. Glinel, S. Demoustier Champagne, B. Nysten, A.M. Jonas, P. Bertrand and S. Yunus, Biosens. Bioelectronn., 26, 4139 (2011).
[17]G.P. Nikoleli, D.P. Nikolelis and C. Methenitis, Anal. Chim. Acta, 675, 58 (2010).
[18]O.Y. Saiapina, V.M. Pyeshkova, O.O. Soldatkin, V.G. Melnik, B.A. Kurc, A. Walcarius, S.V. Dzyadevych and N. Jaffrezic-Renault, Mater. Sci. Eng. C, 31, 1490 (2011).
[19]S. Lee and W. Lee, Bull. Korean Chem. Soc., 23, 1169 (2002).
[20]P.C. Pandey and G. Singh, Talanta, 55, 773 (2001).
[21]N. Batra, M. Tomar, P. Jain and V. Gupta, J. Appl. Phys., 114, 124702 (2013).
[22]J.K. Yang, K.S. Ha, H.S. Baek, S.S. Lee and M.L. Seo, Bull. Korean Chem. Soc., 25, 14999 (2004).
[23]A.S.E. Meibodi and S. Haghjoo, Synth. Met., 194, 1 (2014).
[24]A. Tiwari, S. Aryal, S. Pilla and S. Gong, Talanta, 78, 1401 (2009).
[25]R. Rahmanian and S.A. Mozaffari, Sens. Actuators. B, 207, 772 (2015).
[26]S.A. Mozaffari, H. Salar Amoli, S. Simorgh and R. Rahmanian, Electrochim. Acta 184, 475-482 (2015).
[27]S.A. Mozaffari, T. Chang and S.-M. Park, Biosens. Bioelectron, 26, 74 (2010).
[28]S.A. Mozaffari, T. Chang and S.-M. Park, J. Phys. Chem., C, 113, 12434 (2009).
[29]A.G. Pandolfo and A.F. Hollenkamp, J. Power Sources. 157, 11 (2006).
[30]K.-M. Jin and P. Tsai, Mater. Sci. Eng. B, 139, 81 (2007).
[31]J.R. Macdonald, J. Schoonman and A.P. Lehnen, J. Electroanal. Chem., 131, 77 (1982).
[32]S.A. Mozaffari, R. Rahmanian, M. Abedi and H.S. Amoli, Electrochim. Acta, 146, 538 (2014).
[33]N. Verma and M. Singh, Biosens. Bioelectron., 18, 1219 (2003).
[34]J.H. Jin, S.H. Paek, C.W. Lee, N.K. Min and S.I. Hong, J. Korean Phys. Soc., 42, 735 (2003).
[35]A. Pizzariello, M. Stredansky, S. Stredanska and S. Miertus, Talanta, 54, 763 (2001).
[36]Z. Wu, L. Guan, G. Shen and R. Yu, Analyst., 127, 391 (2002).
[37]Y. Zhengpeng, S. Shihui, D. Hongjuan and Z. Chunjing, Biosens. Bioelectron., 22, 3283 (2007).
[38]R. Sahney, S. Anand, B. Puri and A. Srivastava, Anal. Chim. Acta, 578, 156 (2006).
[39]A. Ali, A.A. Ansari, A. Kaushik, P.R. Solanki, A. Barik, M.K. Pandey and B.D. Malhotra, Mater. Lett., 63, 2473 (2009).
[40]M. Tyagi, M. Tomar and V. Gupta, Biosens. Bioelectron., 41, 110 (2013).
[41] D. Marshal, J. Biosens. Bioelectron., 1, 1 (2010).
[42] I. Kucherenko, O. Soldatkin, B.O. Kasap, S. Öztürk, B. Akata, A. Soldatkin and S. Dzyadevych, Electroanalysis., 24, 1380 (2012).
[43] T. Ahuja, I.A. Mir and D. Kumar, Sens. Actuators. B, 134, 140 (2008).
[44] X. Chen, Z. Yang and S. Si, J. Electroanal. Chem., 635, 1 (2009).
[45]R. Ahmad, N. Tripathy and Y. B. Hahn, Sens. Actuators. B, 194, 290 (2014).